

Contents lists available at ScienceDirect

Physics Letters B

journal homepage: www.elsevier.com/locate/physletb



Resolving the $R_{\rm pA}$ and v_2 puzzle of D^0 mesons in $p{\rm -Pb}$ collisions at the LHC



Chao Zhang a,b,c, Liang Zheng d, Shusu Shi c, Zi-Wei Lin b,*

- ^a School of Science, Wuhan University of Technology, Wuhan, 430070, China
- ^b Department of Physics, East Carolina University, Greenville, NC 27858, USA
- c Institute of Particle Physics, Key Laboratory of Quark&Lepton Physics (MOE), Central China Normal University, Wuhan 430079, China
- ^d School of Mathematics and Physics, China University of Geosciences (Wuhan), Wuhan 430074, China

ARTICLE INFO

Article history: Received 12 May 2023 Received in revised form 25 September 2023 Accepted 27 September 2023 Available colling 4 October 2023

Available online 4 October 2023 Editor: A. Schwenk

ABSTRACT

It has been a challenge to understand the experimental data on both the nuclear modification factor and elliptic flow of D^0 mesons in $p-{\rm Pb}$ collisions at LHC energies. In this work, we study these collisions with an improved multi-phase transport model. By including the independent fragmentation and a significant Cronin effect (i.e., transverse momentum broadening) for charm quarks, we provide the first simultaneous description of the D^0 meson $R_{\rm pA}$ and v_2 data at $p_T \le 8~{\rm GeV}/c$. The model also reasonably describes the D^0 meson p_T spectra and the low- p_T charged hadron spectra, $R_{\rm pA}$ and v_2 . Our results show that both parton interactions and the Cronin effect are important for the D^0 meson $R_{\rm pA}$, while parton interactions are mostly responsible for the D^0 meson v_2 . It is thus essential to include the Cronin effect for the simultaneous description of the D^0 meson $R_{\rm pA}$ and v_2 . This work implies that the Cronin effect could also be important for heavy hadrons in large systems.

© 2023 The Author(s). Published by Elsevier B.V. This is an open access article under the CC BY license (http://creativecommons.org/licenses/by/4.0/). Funded by SCOAP³.

1. Introduction

Heavy flavor hadrons are one of the most important tools to study the perturbative Quantum Chromo-Dynamics (pQCD) in high energy hadronic collisions [1–3]. Over the last two decades, experiments from the Relativistic Heavy Ion Collider (RHIC) and the Large hadron Collider (LHC) [4–7] have collected many data supporting the formation of a hot and dense matter called the quark-gluon-plasma (QGP), and a main goal of high energy heavy ion physics is to study the QGP properties. Heavy quarks provide us a great probe because the heavy quark mass is much larger than the temperature of the dense matter; therefore, heavy flavor particles may only partially thermalize [8] and thus better remember the interaction history with the medium.

Two observables are often measured for heavy flavors in heavy ion collisions: the nuclear modification factor $R_{\rm AA}$ [9–15] and the elliptic flow v_2 [16–22]. Several theoretical models, including the Fokker-Planck approach [23–26] and the relativistic Boltzmann transport approach [27–31], have been developed to study the nuclear suppression and collective flows of heavy flavor hadrons at RHIC and LHC. It has been realized that $R_{\rm AA}$ and v_2 are sensitive to

* Corresponding author. E-mail address: linz@ecu.edu (Z.-W. Lin). the temperature- and energy-dependence of transport properties of the QGP such as the heavy quark diffusion and drag coefficients [32,33]. They are also sensitive to the hadronization mechanisms including quark coalescence and fragmentation [34–39]. Several approaches have shown reasonable agreements with the existing data in large collision systems, suggesting that charm quarks may flow well with the QGP medium due to their frequent interactions with the hot and dense matter [40–42].

Similar measurements of heavy flavor mesons have also been made for small systems like d+ Au collisions at RHIC and p-Pb collisions at LHC in recent years [43–50]. Little to no nuclear suppression $R_{\rm pA}$ but a sizable elliptic flow v_2 has been observed for D^0 mesons in p-Pb collisions at the LHC energies, which has posed a big challenge to theoretical models. One expects that a sizable v_2 comes from significant interactions of charm quarks with the QGP medium, in either hydrodynamics-based models or parton/hadron transport models. On the other hand, a significant interaction of charm quarks with the QGP is expected to inevitably suppress high- p_T charm hadrons [51–53], in contrast to the observed D^0 $R_{\rm pA}$ being almost flat around the value of unity.

Some theoretical studies can reproduce either the heavy meson $R_{\rm pA}$ data [54–60] or v_2 data [61,62]. For example, the POWLANG model [56] can describe the heavy flavor $R_{\rm pA}$ but predicts a small charm v_2 . PQCD calculations that consider cold nuclear medium effects are generally able to describe the charm $R_{\rm pA}$ data [54,55,57,

63], and so is another pQCD model with a parametrized $k_{\rm T}$ broadening [58]. Regarding the heavy flavor elliptic flow, the color glass condensate framework can describe the charm and bottom v_2 in $p-{\rm Pb}$ collisions at LHC [61,62], which indicates the relevance of initial state correlation for heavy quarks in small systems. So far, however, there has not been a simultaneous description of both $R_{\rm pA}$ and v_2 of heavy hadrons. In this study, we investigate the D^0 meson $R_{\rm pA}$ and v_2 in $p-{\rm Pb}$ collisions at LHC energies with an improved version of a multi-phase transport (AMPT) model.

2. Methods

The AMPT model [64,65] is a transport model designed to describe the evolution of the dense matter produced in heavy ion collisions. The string melting version [66] is expected to be applicable when the QGP is formed, as it contains a fluctuated initial condition, partonic scatterings, quark coalescence, and hadronic interactions. Recently, we have developed a new quark coalescence [67], incorporated modern parton distribution functions of the free proton and impact parameter-dependent nuclear shadowing [68], improved heavy flavor productions [69], and applied local nuclear scaling to two input parameters [70]. The AMPT model that we use in this study contains these improvements.

In the string melting version of AMPT model, the excited strings are converted to partons through the string melting mechanism [66]. In particular, the strings are first converted to hadrons through the Lund string fragmentation [71,72], then each hadron is decomposed to partons according to the flavor and spin structures of its valence quarks. Because initial charm quarks are produced from hard pQCD processes during the primary nuclear-nuclear collision, we improve their treatment in this work. Instead of "melting" the initial charm hadrons into charm quarks via string melting, we extract charm quarks produced from the HI-JING model [73] before they enter the Lund string fragmentation. These initial charm quarks then enter the parton cascade; and a charm quark is allowed to interact after its formation time given by $t_{\rm F} = E/m_{\rm T}^2$ [64], where E and $m_{\rm T}$ are the quark energy and transverse mass, respectively.

Since the scattering cross section for charm quarks is in general different from that for light (u,d,s) quarks, we separate the cross section among light quarks (σ_{LQ}) from that between a heavy quark and other quarks (σ_{HQ}) . The default values, $\sigma_{LQ}=0.5$ mb and $\sigma_{HQ}=1.5$ mb, are used unless specified otherwise, and they are determined from a visual fit to the charged hadron v_2 data in p-Pb collisions at 5.02 TeV and D^0 meson v_2 data in p-Pb collisions at 8.16 TeV, respectively. We have also added the independent fragmentation [74] as another hadronization process for heavy quarks, in addition to the usual quark coalescence process [67]. If a heavy quark and its coalescing partner(s) have a large relative distance or a large invariant mass, they are considered to be unsuitable for quark coalescence; instead the heavy quark will hadronize to a heavy hadron via independent fragmentation.

We also include the transverse momentum broadening (i.e., the Cronin effect [75]) for the initial heavy quarks [76,77]. The Cronin effect is often considered as the broadening of the transverse momentum of a produced parton from a hard process due to multiple scatterings of the involved parton(s) in the nucleus [78–81]. Therefore, its strength depends on the number of scatterings a participant (or target) nucleon undergoes while passing the target (or projectile) nucleus [82]. We implement the broadening by adding a transverse momentum kick $k_{\rm T}$ to each $c\bar{c}$ pair in the initial state, where $k_{\rm T}$ is sampled from a two-dimensional Gaussian [76,77,82] with a Gaussian width parameter w:

$$f(\vec{k_{\rm T}}) = \frac{1}{\pi w^2} e^{-k_{\rm T}^2/w^2},\tag{1}$$

$$w = w_0 \sqrt{1 + (n_{\text{coll}} - i)\delta}. \tag{2}$$

Note that a $c\bar{c}$ pair can be produced from either the radiation of one participant nucleon or the collision between one participant nucleon from the projectile and another from the target. In Eq. (2), i=1 for the former case and i=2 for the latter case, while $n_{\rm coll}$ is the number of primary NN collisions of the participant nucleon for the former case and the sum of the numbers of primary NN collisions of both participant nucleons for the latter case. This way, $w=w_0$ for p+p collisions, where

$$w_0 = (0.35 \text{ GeV/c}) \sqrt{b_L^0 (2 + a_L^0)/b_L/(2 + a_L)}.$$
 (3)

In the above, $a_{\rm L}^0=0.5$ and $b_{\rm L}^0=0.9$ GeV $^{-2}$ are the original values in the HIJING1.0 model [73] for the two parameters in the Lund fragmentation function [74], and a_L and b_L are the values in the AMPT model [70]. The dependence of w_0 on the Lund parameters is based on the observation that the average squared transverse momentum of a hadron relative to the fragmenting parent string is proportional to the string tension, which scales as $1/b_{\rm L}/(2+a_{\rm L})$ [64]. We take $a_{\rm L}=0.8$ and determine $b_{\rm L}$ according to the local nuclear thickness functions, where the b_L value is 0.7 GeV^{-2} for p+p collisions but smaller for nuclear collisions [70]. As a result, for p+p collisions, w = 0.375 GeV/c, close to the original value of 0.35 GeV/c for the parameter parj(21) in the HIJING1.0 model [73]. The δ in Eq. (2) controls the strength of the Cronin effect; its default value of $\delta = 5.0$ is determined from comparisons of results of multiple δ values with the D^0 meson $R_{\rm pA}$ data [83]. Note that we follow the usual approach by treating the Cronin effect as the broadening of parton transverse momentum in the initial state. In contrast, the parton cascade represents a final state effect.

In the implementation of the Cronin effect, we give each $c\bar{c}$ pair a transverse boost so that the pair transverse momentum increases by a $\bar{k}_{\rm T}$ sampled from the distribution in Eq. (2). Note that such implementation of the Cronin effect tends to create an artificial peak at mid-rapidity in the rapidity distribution of heavy quarks [77,82,84], since $y = \arcsin(p_{\rm Z}/m_{\rm T})$ will move towards zero after $p_{\rm T}$ increases. Therefore, we choose to keep the rapidity of $c\bar{c}$ pair the same by providing the necessary longitudinal boost after the transverse momentum broadening. We also enforce the momentum conservation of the whole parton system of each event by letting the light (anti)quarks share the opposite value of the total $k_{\rm T}$ given to all $c\bar{c}$ pairs in the event.

3. Results and discussions

Fig. 1 shows in the upper panels our results of the nuclear modification factor R_{pPb} as functions of the transverse momentum for D^0 mesons and charged hadrons in minimum bias p-Pb collisions at 5.02 TeV and 8.16 TeV in comparison with the experimental data. The middle panels show the elliptic flow coefficient v_2 {2} in high multiplicity p-Pb collisions. All results in Fig. 1 are obtained with the full AMPT model, with $\sigma_{I,O} = 0.5$ mb (except for the dot-dashed curves where $\sigma_{LO} = 0.3$ mb), $\sigma_{HO} = 1.5$ mb, and $\delta = 5.0$. We see from panels (a) and (c) that this AMPT model can simultaneously describe the available D^0 meson $R_{\rm pPb}$ data at 5.02 TeV [49] and v_2 data at 8.16 TeV [47] below $p_T \sim 8$ GeV/c. In addition, as shown in panels (b) and (d), the model well describes the charged hadron $R_{\rm pPb}$ [85] and v_2 [86] at 5.02 TeV (solid curves) and reasonably describes the $K_{\rm S}^0$ v_2 at 8.16 TeV [47] below $p_{\rm T}\sim 1$ GeV/c. Furthermore, panels (e) and (f) show the D^0 meson and charged hadron p_T spectra in minimum bias p-Pb and p+p collisions at 5.02 TeV. We see that the AMPT model can well describe the D^0 p_T spectra data [49] in both p+p and p-Pb systems, while the agreements with the charged hadron p_T spectra data [85] are reasonable below $p_{\rm T} \sim 1.5~{\rm GeV}/c$.

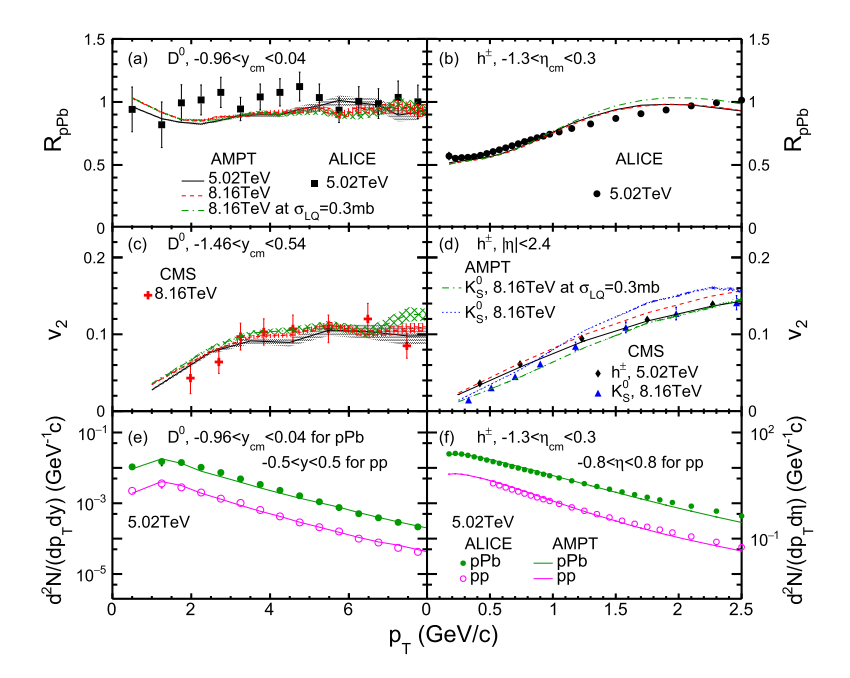


Fig. 1. $R_{\rm pPb}$ of (a) D^0 mesons and (b) charged hadrons in minimum bias $p-{\rm Pb}$ collisions, v_2 of (c) D^0 mesons, (d) charged hadrons and $K_{\rm S}^0$ in high multiplicity $p-{\rm Pb}$ collisions, and the $p_{\rm T}$ spectra of (e) D^0 mesons and (f) charged hadrons in minimum bias $p-{\rm Pb}$ and p+p collisions at 5.02 TeV from the improved AMPT model in comparison with the experimental data around mid-rapidity.

In our analysis, we follow the exact procedures of the ALICE and CMS experiments [47,49,85,86]. Specifically, the D^0 meson and charged hadron nuclear modification factors are analyzed for minimum bias collisions within $-0.96 < y_{\rm cm} < 0.04$ and $-1.3 < \eta_{\rm cm} < 0.3$, respectively. The elliptic flow coefficient is analyzed for high multiplicity $p-{\rm Pb}$ events within $N_{\rm track} \in [185-220)$ at $5.02~{\rm TeV}$ and $N_{\rm track} \in [185-250)$ at $8.16~{\rm TeV}$, where $N_{\rm track}$ is the number of charged hadrons with $p_{\rm T} > 0.4~{\rm GeV}/c$ within $|\eta| < 2.4$. To calculate the elliptic flow from two-particle correlations, we apply $|\Delta \eta| > 2$ at $5.02~{\rm TeV}$ and $|\Delta \eta| > 1$ at $8.16~{\rm TeV}$, where charged hadrons are selected within $|\eta| < 2.4$ while D^0 and K_S^0 mesons are within $-1.46 < y_{\rm cm} < 0.54$. The elliptic flow $v_2\{2\}$, written as v_2 for brevity, is calculated as [47,86]

$$v_2(\text{tri}) = V_{2\Delta}(\text{tri}, \text{ref}) / \sqrt{V_{2\Delta}(\text{ref}, \text{ref})}, \tag{4}$$

where "tri" represents the trigger particle of interest, and "ref" represents a reference charged hadron with $0.3 < p_{\rm T} < 3.0$ GeV/c. Note that in this study the result of a particle species represents the average of the particle and its corresponding anti-particle; also, all the rapidity and η cuts refer to their values in $p{\rm -Pb}$ (not Pb-p) collisions.

Since the available data on D^0 mesons are the $R_{\rm pPb}$ at 5.02 TeV and v_2 at 8.16 TeV, we also show in Fig. 1(a) and (c) the predictions of R_{pPb} at 8.16 TeV (dashed curve) and v_2 at 5.02 TeV (solid curve). We see that the $R_{\rm pPb}$ results are almost the same at the two energies but v_2 shows an increase with the colliding energy. This is also the case for the charged hadron $R_{\rm pPb}$ and v_2 , as shown by the dashed curves for 8.16 TeV in Fig. 1(b) and (d). We note that the model overestimates the v_2 of K_S^0 mesons at 8.16 TeV when $\sigma_{LQ} = 0.5$ mb, which well reproduces the charged hadron v_2 at 5.02 TeV, is used. On the other hand, the parton scattering cross section σ could be different at different energies. For example, the shear viscosity-to-entropy ratio satisfies $\eta/s \propto 1/(n^{2/3}\sigma)$ for a parton gas in equilibrium under isotropic scatterings [87,88], where n is the parton number density. As a result, for the simple case of a constant η/s , σ would be smaller at higher densities. For anisotropic scatterings, which is the case for the AMPT model, the

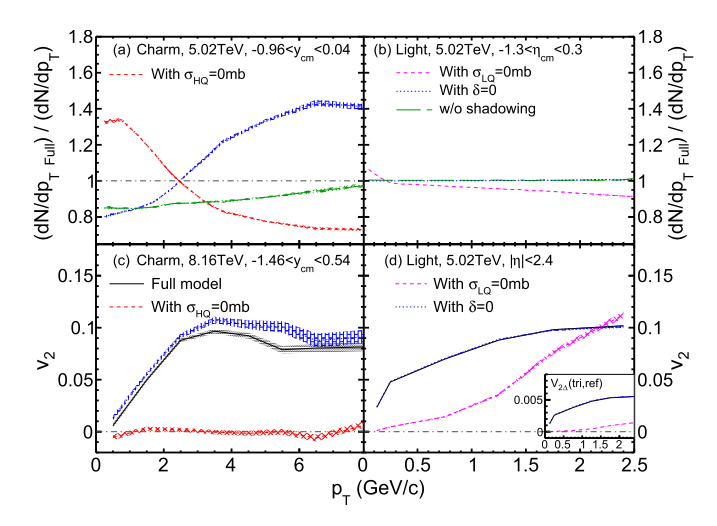


Fig. 2. Ratio of the p_T spectrum from the full AMPT model over that from the AMPT model with a different test configuration for (a) charm quarks and (b) light quarks in p-Pb collisions at 5.02 TeV, (c) v_2 of charm quarks at 8.16 TeV, and (d) v_2 of light quarks at 5.02 TeV from the AMPT model for p-Pb collisions. The Cronin effect is turned off with $\delta=0$. The inset in panel (d) shows the light quark $V_{2\Delta}(\text{tri}, \text{ref})$.

relationship between η/s and σ is more complicated but qualitatively similar [88]. In addition, high temperature pQCD results [89] show that σ should depend on the temperature since the Debye screening mass is temperature-dependent. Therefore, we have also explored the effect of a different light quark cross section. As shown by the dot-dashed curves in Fig. 1(a)-(d), changing σ_{LQ} from 0.5 mb to 0.3 mb at 8.16 TeV enables the AMPT model to well reproduce the K_S^0 v_2 data, but this change has almost no effect on the D^0 meson R_{pPb} and v_2 . As expected, the smaller σ_{LQ} leads to a small enhancement of the charged hadron R_{pPb} , as shown in Fig. 1(b).

We now separately turn off various effects to identify the key ingredients that allow the improved AMPT model to simultaneously describe the D^0 meson $R_{\rm pPb}$ and v_2 . Fig. 2(a) shows the ratio of the charm quark $p_{\rm T}$ spectrum from the full AMPT model over

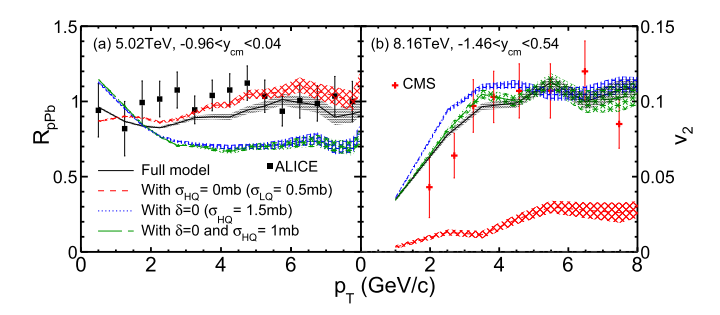


Fig. 3. (a) $R_{\rm pPb}$ at 5.02 TeV and (b) v_2 at 8.16 TeV for D^0 mesons in p-Pb collisions from the full AMPT model (solid), the model without charm quark scatterings (dashed), the model without the Cronin effect for charm quarks (dotted), and the model without the Cronin effect at a smaller charm quark scattering cross section (long-dashed) in comparison with the experimental data (symbols).

that from different test configurations of the AMPT model for minimum bias p-Pb collisions at 5.02 TeV, while Fig. 2(b) shows the ratios for light quarks. The dashed curves in panels (a) and (c) represent the results of charm quarks without charm quark scatterings (but with scatterings among light quarks), while the dashed curves in panel (b) and (d) represent the light quark results without scatterings among light quarks. We see that parton scatterings suppress the parton yield at relatively high p_T (and enhance the yield at low $p_{\rm T}$) due to the parton energy loss or jet quenching [51,90]; this effect is especially significant for charm quarks, partially due to the larger scattering cross section for charm quarks. From the dotted curves that correspond to turning off the charm Cronin effect, we find that the Cronin effect significantly enhances the charm quark yield at relatively high p_T and essentially cancels out the effect from jet quenching. In addition, we see that the EPS09s nuclear shadowing [68] has almost no effect on the light quark p_T spectrum but a modest suppression effect on the charm quark p_T spectrum in the transverse momentum range shown in Fig. 2.

We show in Fig. 2(c) and (d) the results on the charm quark v_2 at 8.16 TeV and the light quark v_2 at 5.02 TeV, respectively, for the high multiplicity p-Pb collisions. From the dashed curves, we see that the charm quark v_2 is mostly generated from the scatterings of charm quarks with the medium, while the initial state correlation before rescatterings (or non-flow) contributes significantly to the light quark v_2 but little to the charm quark v_2 . We also see that the Cronin effect for charm quarks modestly suppresses the charm quark v_2 ; it has little effect on the light quark v_2 , as expected. Note that in Fig. 2(d) the light quark $v_2(p_T)$ without scatterings among light quarks is even higher than that with parton scatterings at $p_T > 2.2$ GeV/c. The inset in Fig. 2(d) shows the corresponding numerator, $V_{2\Delta}(tri, ref)$, for the light quark v_2 , where the result without scatterings is significantly lower than that with parton scatterings, as expected. Therefore, the relatively high $v_2(p_T)$ without scatterings is due to the fact that the denominator $\sqrt{V_{2\Delta}(ref, ref)}$ in Eq. (4), which corresponds to the reference elliptic flow, is much smaller without scatterings.

We now examine the effects of transverse momentum broadening and parton scatterings on the D^0 meson $R_{\rm pPb}$ and v_2 . When the Cronin effect is turned off (with $\delta=0$), we see in Fig. 3(a) that the D^0 $R_{\rm pPb}$ is significantly suppressed at high $p_{\rm T}$ but enhanced at low $p_{\rm T}$. Therefore, the Cronin effect is very important for the D^0 meson $R_{\rm pPb}$. In addition, parton scatterings (at $\sigma_{\rm HQ}=1.5$ mb) are seen to suppress the D^0 meson $R_{\rm pPb}$ at high $p_{\rm T}$, qualitatively the same as its effect on charm quarks as shown in Fig. 2(a). Quantitatively, the effect of parton scatterings on the D^0 meson $R_{\rm pPb}$ is smaller than that on charm quarks; this is because the fraction of charm quarks hadronizing via quark coalescence (instead of fragmentation) increases with the amount of scatterings and consequently the system size. When charm quark scatterings are

turned off (dashed curve) in the AMPT model, the charm quark yield at high $p_{\rm T}$ is enhanced due to the absence of energy loss. On the other hand, more charm quarks hadronize via independent fragmentation (than the case with charm quark scatterings), which reduces the enhancement of D^0 mesons at high $p_{\rm T}$.

In Fig. 3(b), the D^0 meson v_2 is mostly very small when charm quark scatterings are turned off (dashed curve); the $D^0 v_2$ is thus mostly generated by parton scatterings, similar to the charm quark v_2 shown in Fig. 2(c). Note that, even if charm quarks have zero v_2 , the D^0 v_2 can be finite since it has a contribution from the light quark v_2 through quark coalescence [34]. In the AMPT model without the Cronin effect, the D^0 meson v_2 (dotted curve) is slightly higher. Therefore, the Cronin effect modestly suppresses the $D^0 v_2$. We have also decreased the charm quark scattering cross section to 1.0 mb, from the default value of 1.5 mb in the full model, to better fit the D^0 meson v_2 (long-dashed curve). The corresponding D^0 meson $R_{\rm pA}$ result is shown in Fig. 3(a) as the long-dashed curve, which is seen to still severely underestimates the data at high $p_{\rm T}$. The Cronin effect is thus crucial for the simultaneous description of the D^0 meson $R_{\rm pPb}$ and v_2 data according our model calculations.

Many previous theoretical methods and phenomenological models have found the Cronin effect to be important. For example, pQCD results [76] have indicated that the Cronin effect is needed to describe the experiment data of open heavy flavors at fixedtarget energies. In the pQCD-based HVQMNR code [77,82], transverse momentum broadening is also needed to describe quarkonium p_T distributions and heavy flavor azimuthal distributions from fixed-target to LHC energies. In the HVQMNR code, a transverse momentum kick in the form of Eq. (2) is applied to each produced heavy quark in p+p collisions, where the Gaussian width is energy-dependent [77]: $\langle k_T^2 \rangle_p = [1 + \ln(\sqrt{s_{NN}}/20/\text{GeV})/n] \text{ GeV}^2$ with n=12 for J/ψ productions. For minimum-bias p+A collisions, the Gaussian width increases to $\langle k_{\rm T}^2 \rangle_A = \langle k_{\rm T}^2 \rangle_p + \delta k_{\rm T}^2$ [82], where $\delta k_{\rm T}^2 = (1.5 \rho_0 R_A \sigma_{pp}^{in} - 1) \Delta^2(\mu)$. Here, $R_A = 1.2 A^{1/3}$ fm represents the nuclear radius, $\rho_0 = 0.16/\text{fm}^3$ is the average nuclear density, σ_{pp}^{in} is the inelastic p+p cross section, and $\Delta(\mu)=0.318\,\text{GeV}$ for charm productions at $\mu = 2m_c = 2.54 \,\text{GeV}$ [82]. Note that we apply the broadening to each $c\bar{c}$ pair, while the HVQMNR code applied it to each charm (anti)quark after the charm pair production [91]; therefore, we have calculated the k_T broadening to each charm quark in the comparisons below. For p+p collisions at 5.02 TeV, the HVQMNR code [82,92] gives $\langle k_T^2 \rangle = 1.46 \,\text{GeV}^2$, higher than our value of $0.04 \,\text{GeV}^2$. For minimum bias p-Pb collisions at 5.02TeV, the HVQMNR code gives $\langle k_T^2 \rangle = 2.50 \,\text{GeV}^2$, lower than our value of $3.27 \,\text{GeV}^2$.

The AMPT model currently only includes the collisional energy loss via two-body elastic parton scatterings, while the parton radiative energy loss is not included. In the relativistic limit, the heavy quark collisional energy loss has been shown to depend on the path length L linearly while the radiative energy loss scales as L^2 [93]. Therefore, the collisional energy loss of charm quarks is expected to be more important than the radiative energy loss for small systems like p-Pb, although the p_T scale below which the collisional energy loss dominates is model-dependent [38,94-96]. In addition, the radiative energy loss of charm quarks through inelastic collisions would suppress the charm p_T spectrum at high p_{T} , qualitatively the same as the collisional energy loss through elastic collisions. Therefore, the inclusion of the charm quark radiative energy loss would not change our conclusion that the Cronin effect is needed to compensate for the effect of energy loss and consequently describe the observed D^0 meson R_{pPb} and v_2 simultaneously. We also note that our σ_{HO} value is much larger than that expected from pQCD with a typical screening mass. However, high temperature pQCD results are known to be quantitatively un-

reliable at low to moderate temperatures. For example, the shear viscosity of the quark gluon plasma expected from pQCD with thermal screening masses is much higher [97] than that extracted from a Bayesian analysis of the experimental data [98]. Therefore, we treat the magnitudes of parton cross sections as free parameters in the AMPT model and determine them from comparisons with the experimental data.

Since the Cronin effect is expected to be stronger for a larger collision system, our study also suggests that it would be important to include the Cronin effect in studies of light hadron [99] or heavy hadron $R_{\rm AA}$ [24] in large systems. Currently, several models are able to reasonably describe the D meson $R_{\rm AA}$ and v_2 [31,39,40,42]. The inclusion of the Cronin effect may change the model results and affect the extracted values of the charm quark transport coefficients. Therefore, further studies, including those with a predicted (instead of a fit) strength for the Cronin effect and those on charmonium observables, will lead to a better understanding of the roles of cold nuclear matter and hot medium effects on heavy flavor productions in small to large collision systems

4. Summary

We have studied the D^0 meson as well as charged hadron nuclear modification factor $R_{\rm pPb}$ in minimum bias $p{\rm -Pb}$ collisions and elliptic flow v_2 in high multiplicity p-Pb collisions at LHC energies with a multi-phase transport model. After improving the model with the transverse momentum broadening (i.e., the Cronin effect) and independent fragmentation for charm quarks, we are able to provide the first simultaneous description of both the $R_{\rm pPb}$ and v_2 data of D^0 mesons below the transverse momentum of 8 GeV/c. In addition, the transport model reasonably describes the D^0 meson p_T spectra in both p-Pb and p+p collisions and the low- p_T charged hadron p_T spectra, R_{pPb} and v_2 . We find that both parton scatterings and the Cronin effect significantly affect the D^0 meson $R_{\rm nPh}$. On the other hand, the D^0 meson v_2 is mostly generated by parton scatterings, while the Cronin effect leads to a modest reduction of the charm v_2 . In particular, we demonstrate the importance of the Cronin effect for resolving the D^0 meson $R_{\rm pPb}$ and v_2 puzzle at LHC energies. Since the Cronin effect is expected to grow with the system size, this study also implies the importance of including the Cronin effect in studies of heavy hadron R_{AA} and v_2 in large systems.

Declaration of competing interest

The authors declare that they have no known competing financial interests or personal relationships that could have appeared to influence the work reported in this paper.

Data availability

No data was used for the research described in the article.

Acknowledgement

We thank Jacek Otwinowski for the clarification about the ALICE trigger. This work is supported by the National Key Research and Development Program of China under contract Nos. 2022YFA1604900 and 2020YFE0202002 (C.Z. and S.S.), the National Natural Science Foundation of China under Grant Nos. 12175084, 11890710 (11890711) (C.Z. and S.S.) and 11905188 (L.Z.), the Chinese Scholarship Council No. 201906770050 (C.Z.), and the National Science Foundation under Grant No. 2012947 and No. 2310021 (Z.-W.L.). ZWL thanks the Institute for Nuclear Theory at

the University of Washington for its kind hospitality and discussions with Ramona Vogt and Peter Petreczky during the revision of this work.

References

- [1] H. van Hees, V. Greco, R. Rapp, Phys. Rev. C 73 (2006) 034913.
- [2] N. Brambilla, et al., Eur. Phys. J. C 71 (2011) 1534.
- [3] A. Andronic, et al., Eur. Phys. J. C 76 (2016) 107.
- [4] M. Gyulassy, L. McLerran, Nucl. Phys. A 750 (2005) 30.
- [5] J. Adams, et al., STAR, Nucl. Phys. A 757 (2005) 102.
- [6] K. Adcox, et al., PHENIX, Nucl. Phys. A 757 (2005) 184.
- [7] B. Muller, J. Schukraft, B. Wyslouch, Annu. Rev. Nucl. Part. Sci. 62 (2012) 361.
- [8] G.D. Moore, D. Teaney, Phys. Rev. C 71 (2005) 064904.
- [9] L. Adamczyk, et al., STAR, Phys. Rev. Lett. 113 (2014) 142301, Erratum: Phys. Rev. Lett. 121 (2018) 229901.
- [10] A.M. Sirunyan, et al., CMS, Phys. Lett. B 782 (2018) 474.
- [11] S. Acharya, et al., ALICE, J. High Energy Phys. 10 (2018) 174.
- [12] J. Adam, et al., STAR, Phys. Rev. C 99 (2019) 034908.
- [13] S. Acharya, et al., ALICE, J. High Energy Phys. 01 (2022) 174.
- [14] S. Acharya, et al., ALICE, Phys. Lett. B 839 (2023) 137796.
- [15] S. Acharya, et al., ALICE, Phys. Lett. B 827 (2022) 136986.
- [16] B. Abelev, et al., ALICE, Phys. Rev. Lett. 111 (2013) 102301.
- [17] L. Adamczyk, et al., STAR, Phys. Rev. Lett. 118 (2017) 212301.
- [18] S. Acharya, et al., ALICE, Phys. Rev. Lett. 120 (2018) 102301.
- [19] A.M. Sirunyan, et al., CMS, Phys. Rev. Lett. 120 (2018) 202301.
- [20] S. Acharya, et al., ALICE, Phys. Rev. Lett. 120 (2018) 102301.
- [21] S. Acharya, et al., ALICE, J. High Energy Phys. 10 (2020) 141.
- [22] S. Acharya, et al., ALICE, Phys. Lett. B 813 (2021) 136054.
- [23] S.K. Das, J.-E. Alam, P. Mohanty, Phys. Rev. C 82 (2010) 014908.
- [24] M. He, R.J. Fries, R. Rapp, Phys. Rev. Lett. 110 (2013) 112301.
- [25] S.S. Cao, G.Y. Qin, S.A. Bass, Phys. Rev. C 92 (2015) 024907.
- [26] T. Lang, H. van Hees, G. Inghirami, J. Steinheimer, M. Bleicher, Phys. Rev. C 93 (2016) 014901.
- [27] O. Fochler, Z. Xu, C. Greiner, Phys. Rev. C 82 (2010) 024907.
- [28] M. Djordjevic, M. Djordjevic, Phys. Lett. B 734 (2014) 286.
- [29] J.C. Xu, J.F. Liao, M. Gyulassy, J. High Energy Phys. 02 (2016) 169.
- [30] T.S. Song, H. Berrehrah, D. Cabrera, W.G. Cassing, E. Bratkovskaya, Phys. Rev. C 93 (2016) 034906.
- [31] S.S. Cao, T. Luo, G.Y. Qin, X.N. Wang, Phys. Rev. C 94 (2016) 014909.
- [32] S.K. Das, F. Scardina, S. Plumari, V. Greco, Phys. Lett. B 747 (2015) 260.
- [33] A. Beraudo, et al., Nucl. Phys. A 979 (2018) 21.
- [34] Z.-W. Lin, D. Molnar, Phys. Rev. C 68 (2003) 044901.
- [35] V. Greco, C.M. Ko, R. Rapp, Phys. Lett. B 595 (2004) 202.
- [36] Y. Oh, C.M. Ko, S.H. Lee, S. Yasui, Phys. Rev. C 79 (2009) 044905.
- [37] M. He, R.J. Fries, R. Rapp, Phys. Rev. C 86 (2012) 014903.
- [38] S.S. Cao, G.Y. Qin, S.A. Bass, Phys. Rev. C 88 (2013) 044907.
- [39] T. Song, H. Berrehrah, D. Cabrera, J.M. Torres-Rincon, L. Tolos, W. Cassing, E. Bratkovskaya, Phys. Rev. C 92 (2015) 014910.
- [40] F. Scardina, S.K. Das, V. Minissale, S. Plumari, V. Greco, Phys. Rev. C 96 (2017) 044905.
- [41] S. Cao, et al., Phys. Rev. C 99 (2019) 054907.
- [42] M. He, R. Rapp, Phys. Rev. Lett. 124 (2020) 042301.
- [43] J. Adams, et al., STAR, Phys. Rev. Lett. 94 (2005) 062301.
- [44] A. Adare, et al., PHENIX, Phys. Rev. Lett. 112 (2014) 252301.
- [45] B.B. Abelev, et al., ALICE, Phys. Rev. Lett. 113 (2014) 232301.
- [46] R. Aaij, et al., LHCb, J. High Energy Phys. 10 (2017) 090.
- [47] A.M. Sirunyan, et al., CMS, Phys. Rev. Lett. 121 (2018) 082301.[48] A.M. Sirunyan, et al., CMS, Phys. Lett. B 791 (2019) 172.
- [46] A.W. Shunyan, et al., CMS, Phys. Lett. B 791 (2019) 172.

 [49] S. Acharya, et al., ALICE, J. High Energy Phys. 12 (2019) 092.
- [50] S. Acharya, et al., ALICE, Phys. Rev. C 104 (2021) 054905.
- [51] Y. Xu, S. Cao, G.-Y. Qin, W. Ke, M. Nahrgang, J. Auvinen, S.A. Bass, Nucl. Part. Phys. Proc. 276–278 (2016) 225.
- [52] X. Du, R. Rapp, J. High Energy Phys. 03 (2019) 015.
- [53] S. Cao, X.-N. Wang, Rep. Prog. Phys. 84 (2021) 024301.
- [54] H. Fujii, K. Watanabe, Nucl. Phys. A 920 (2013) 78.
- [55] Z.-B. Kang, I. Vitev, E. Wang, H. Xing, C. Zhang, Phys. Lett. B 740 (2015) 23.
- [56] A. Beraudo, A. De Pace, M. Monteno, M. Nardi, F. Prino, J. High Energy Phys. 03 (2016) 123.
- [57] J.H. Liu, S. Plumari, S.K. Das, V. Greco, M. Ruggieri, Phys. Rev. C 102 (2020) 044902.
- [58] S.K. Tripathy, M. Younus, S. De, arXiv:2008.05265 [hep-ph], 2020.
- [59] G.S.d. Santos, M.V.T. Machado, G.G. da Silveira, Eur. Phys. J. C 82 (2022) 795.
- [60] W. Ke, I. Vitev, Phys. Rev. C 107 (2023) 064903.
- [61] C. Zhang, C. Marquet, G.Y. Qin, S.Y. Wei, B.W. Xiao, Phys. Rev. Lett. 122 (2019) 172302.
- [62] C. Zhang, C. Marquet, G.Y. Qin, Y. Shi, L. Wang, S.Y. Wei, B.W. Xiao, Phys. Rev. D 102 (2020) 034010.
- [63] J. Adam, et al., ALICE, Phys. Rev. C 94 (2016) 054908.

- [64] Z.-W. Lin, C.M. Ko, B.A. Li, B. Zhang, S. Pal, Phys. Rev. C 72 (2005) 064901.
- [65] Z.-W. Lin, L. Zheng, Nucl. Sci. Tech. 32 (2021) 113.
- [66] Z.-W. Lin, C.M. Ko, Phys. Rev. C 65 (2002) 034904.
- [67] Y.C. He, Z.-W. Lin, Phys. Rev. C 96 (2017) 014910.
- [68] C. Zhang, L. Zheng, F. Liu, S.S. Shi, Z.-W. Lin, Phys. Rev. C 99 (2019) 064906.
- [69] L. Zheng, C. Zhang, S.S. Shi, Z.-W. Lin, Phys. Rev. C 101 (2020) 034905.
- [70] C. Zhang, L. Zheng, S. Shi, Z.-W. Lin, Phys. Rev. C 104 (2021) 014908.
- [71] B. Andersson, G. Gustafson, G. Ingelman, T. Sjostrand, Phys. Rep. 97 (1983) 31.
- [72] B. Andersson, G. Gustafson, B. Soderberg, Z. Phys. C 20 (1983) 317.
- [73] X.-N. Wang, M. Gyulassy, Phys. Rev. D 44 (1991) 3501.
- [74] T. Sjostrand, Comput. Phys. Commun. 82 (1994) 74.
- [75] J.W. Cronin, H.J. Frisch, M.J. Shochet, J.P. Boymond, R. Mermod, P.A. Piroue, R.L. Sumner, E100, Phys. Rev. D 11 (1975) 3105.
- [76] M.L. Mangano, P. Nason, G. Ridolfi, Nucl. Phys. B 405 (1993) 507.
- [77] R. Vogt, Phys. Rev. C 98 (2018) 034907.
- [78] B.Z. Kopeliovich, J. Nemchik, A. Schafer, A.V. Tarasov, Phys. Rev. Lett. 88 (2002) 232303.
- [79] D. Kharzeev, Y.V. Kovchegov, K. Tuchin, Phys. Rev. D 68 (2003) 094013.
- [80] I. Vitev, T. Goldman, M.B. Johnson, J.W. Qiu, Phys. Rev. D 74 (2006) 054010.
- [81] A. Accardi, arXiv:hep-ph/0212148, 2002.
- [82] R. Vogt, Phys. Rev. C 103 (2021) 035204.

- [83] C. Zhang, Z.-W. Lin, L. Zheng, S. Shi, in: Hard Probes 2023, 2023, arXiv:2309. 01215 [nucl-th].
- [84] R. Vogt, Phys. Rev. C 101 (2020) 024910.
- [85] S. Acharya, et al., ALICE, J. High Energy Phys. 11 (2018) 013.
- [86] S. Chatrchyan, et al., CMS, Phys. Lett. B 724 (2013) 213.
- [87] P. Huovinen, D. Molnar, Phys. Rev. C 79 (2009) 014906.
- [88] N.M. MacKay, Z.-W. Lin, Eur. Phys. J. C 82 (2022) 918.
- [89] P.B. Arnold, G.D. Moore, L.G. Yaffe, J. High Energy Phys. 05 (2003) 051.
- [90] V. Ozvenchuk, J. Aichelin, P.B. Gossiaux, B. Guiot, M. Nahrgang, K. Werner, J. Phys. Conf. Ser. 779 (2017) 012033.
- [91] R. Vogt, in: PoS HardProbes2020, 2021, p. 053.
- [92] R. Vogt, Phys. Rev. C 106 (2022) 025201.
- [93] M.G. Mustafa, Phys. Rev. C 72 (2005) 014905.
- [94] M. Nahrgang, J. Aichelin, P.B. Gossiaux, K. Werner, Phys. Rev. C 90 (2014) 024907.
- [95] W. Ke, Y. Xu, S.A. Bass, Phys. Rev. C 100 (2019) 064911.
- [96] W. Ke, X.-N. Wang, J. High Energy Phys. 05 (2021) 041.
- [97] L.P. Csernai, J.I. Kapusta, L.D. McLerran, Phys. Rev. Lett. 97 (2006) 152303.
- [98] D. Everett, et al., JETSCAPE, Phys. Rev. C 103 (2021) 054904.
- [99] I. Vitev, M. Gyulassy, Phys. Rev. Lett. 89 (2002) 252301.